17th World Conference on Earthquake Engineering, 17WCEE
Sendai, Japan - September 13th to 18th 2020

PREDICTIVE FIBER MODEL FOR REBAR BUCKLING

D. Sosa [1], M. Kowalsky [2]

[1] *Assistant Professor, Escuela Politécnica Nacional, Ph.D. Candidate, North Carolina State University, dasosaca@ncsu.edu*
[2] *Christopher W. Clark Distinguished Professor of Structural Engineering, North Carolina State University, kowalsky@ncsu.edu*

Abstract

Rebar buckling is a damage control limit state in reinforced concrete (RC) columns, and it needs an accurate and reliable definition for structural assessment. While rebar buckling has been extensively studied for individual bars tested in compression or cyclic loading, these previous experiments do not capture the real boundary conditions that represent the buckling phenomenon in RC columns. Additionally, other experimental studies have evaluated the influence of rebar buckling on the global response of real columns, but they could not measure the local response of longitudinal and transverse steel reinforcement in the plastic hinge region. Furthermore, 3D FE models used to predict rebar buckling in columns are computationally expensive and have limited applicability. Accordingly, the current understanding of rebar buckling could be improved in three aspects: use of data from tests with real boundary conditions, experimental measurements of the local response, and efficient computational models. Global and local data measured with a non-contact monitoring instrumentation was provided from a subset of 20 RC columns performed at NC State. This dataset, involving quasi-static experiments, established a robust standard for evaluating rebar buckling under lateral cyclic loading. Lastly, this research proposes a new procedure to define the plastic hinge region of RC columns using fiber models. The approach predicts the rebar buckling phenomenon based on deformation compatibility, nonlinear material properties, and geometric nonlinearities. The new procedure proposes a plastic hinge region where the steel reinforcement is composed of discrete fiber elements, and sectional compatibility with the concrete core is enforced through constraints. Furthermore, the new method is validated with the experimental dataset. Four characteristics of evaluation were used: the maximum force-displacement ordinate, the minimum force-displacement ordinate, the energy dissipated, and local strain histories. In conclusion, this research validates, with global and local experimental data, the accuracy of the new procedure to predict rebar buckling in RC columns based on fiber models. This validation shows that buckled rebar does not behave as a uniaxial fiber, but rather as individual fiber elements subjected to axial and bending strains. Moreover, the fiber model implemented in this study is less computationally expensive than 3D FE models, so it can be used in the future to evaluate rebar buckling in nonlinear time history analysis.

Keywords: rebar buckling; fiber model; reinforced concrete; prediction.

1. Introduction

In high seismic regions, reinforced concrete (RC) elements under axial and flexural deformations will experience rebar buckling for large displacement demands. The most common examples of rebar buckling have been observed in RC bridge columns after strong ground motions, but rebar buckling can happen in any RC element that combines lateral cyclic loading and compression forces. In Performance-Based Seismic Engineering (PBSE), rebar buckling defines the damage control limit state of RC structures, and this phenomenon can be used as an engineering measurement to determine if a structural retrofit or repair is feasible. Nevertheless, rebar buckling is a complex phenomenon to represent and predict, so a complete agreement on the definition of the rebar buckling limit state has not been achieved.

Researchers have studied the rebar buckling phenomenon with analytical and experimental approaches, and these studies have been applied to single rebar and complete RC elements to improve the

understanding of this limit state. For example, [1] studied buckling due to inelastic axial compression and geometrical nonlinearity based on FE microanalysis of single rebar. Later, [2] developed cyclic stress-strain relationships for rebar with the inclusion of the buckling influence based on the results obtained in [1]. Additionally, [3] used stability analysis to develop prediction models for the buckling length of rebar supported by many ties. Moreover, the previous stress-strain rebar model developed by [2] has been updated recently by [4]. Indeed, current constitutive materials and fiber models can include the effect of inelastic rebar buckling in RC elements [5], but they cannot predict this phenomenon. Finally, [6], [7], and [8] have shown that sophisticated 3D FE models can predict rebar buckling in RC columns under monotonic compressive loads, monotonic pushover, and cyclic pushover, but 3D FE models tend to sacrifice computational efficiency.

Analytical approaches for rebar buckling are based on experimental observations, for experimental studies have discovered the most important aspects that trigger the rebar buckling phenomenon. For example, [9] and [10] noticed that rebar buckling is highly influenced by the cyclic loading pattern and the magnitude of tensile strain in the rebar. Additionally, [11] identified four main features for rebar buckling: reverse loading, high levels of tensile strain, gradual accumulation strain, and buckling under compression force. Moreover, [12] and [13] studied the influence of initial eccentricities and rebar aspect ratio, and [12] was one of the first studies to state that buckling always happens in the weak axis of the rebar. Finally, [14] conducted an extensive experimental study of rebar buckling in RC bridge columns with non-contact monitoring instrumentation that captured the global response of the columns and the local strain response of the rebar.

In general, experimental observations have shown that cyclic loading and boundary conditions between rebar and concrete core are parameters that highly influence the rebar buckling phenomenon. Indeed, these parameters are not fully represented in some analytical models, so expensive computational models are needed to obtain a solution for this phenomenon. This paper proposes an efficient computational fiber model that predicts rebar buckling in RC circular columns under cyclic loading based on deformation compatibility, nonlinear constitutive models, and geometric nonlinearities.

2. Method

This section includes the description of the experimental data provided by [14] which is going to be used as reference to validate the Predictive Fiber Model (PFM) for rebar buckling. Additionally, a detailed description of the components and conditions used in the PFM is presented, so the application of this procedure can be easily implemented in any software that uses the fiber method approach.

2.1 Experimental data set

The data set provided by [14] consists of 20 real scale columns tested with a cyclic pushover procedure and monitored by a non-contact position measurement system [15]. This camera system reads the location of the target marker attached to the rebar in three-dimensional coordinates in real-time during the test. Through geometric relationships, strains at the longitudinal reinforcement edge can be determined from the target marker locations.

The data presented in [14] characterizes an experimental study of circular RC columns under lateral displacement demand in which they determine capacity curves, rebar strain hysteresis, vertical strain profiles, cross-section curvatures, curvature distribution, and fixed end rotations due to strain penetration. For this paper, the capacity curves are considered to validate the global response of the model, and the rebar strain hysteresis curves are used to validate the local response of the buckled rebar. The capacity curve plots the column displacement at the top versus the shear at the base of the column, and the rebar hysteresis shows the relation between the column displacement at the top versus the rebar strain in the middle of two markers. For example, Fig. 1 presents the two experimental relations that this paper uses to validate the PFM.

Column [14]

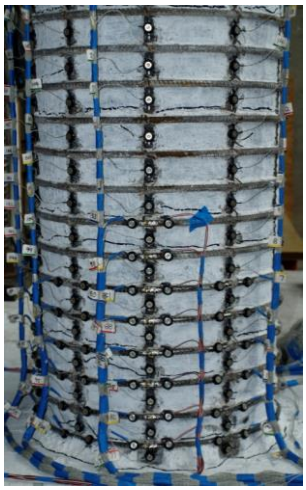

Markers [14]

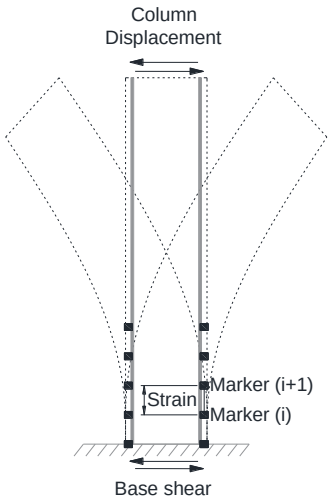

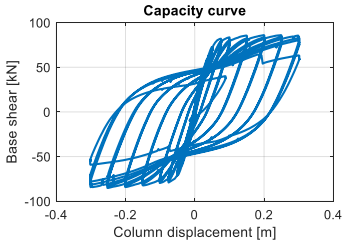

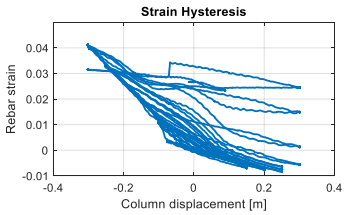

Fig. 1 – Experimental relations

The rebar buckling phenomenon can be observed in the strain hysteresis curve when the rebar has tensile strain under compression axial force [14]. The cyclic lateral displacement at the top of the column produces cyclic loading on the rebar from tension to compression, and during most of the experimental measurements, the rebar under compression forces has compression strains. However, after many cycles of large displacement, the rebar has a jump from compression strain to tensile strain for the same level of column displacement (see Fig. 2), which can be attributed to the rebar buckling phenomenon. The markers on the rebar are located at the edge of the rebar, so the markers are measuring an edge fiber. Furthermore, the buckled rebar has axial and flexural deformation, so the jump on the edge strain happens when the tensile strain due to flexural deformation is larger than the compression strain due to axial deformation. This study considers three types of coordinates in strain hysteresis curves: type 1 is tensile strain under tension force, type 2 is compression strain under compression force, and type 3 is tensile strain under compression force. The PFM should be able to predict all of these types of coordinates for the local response.

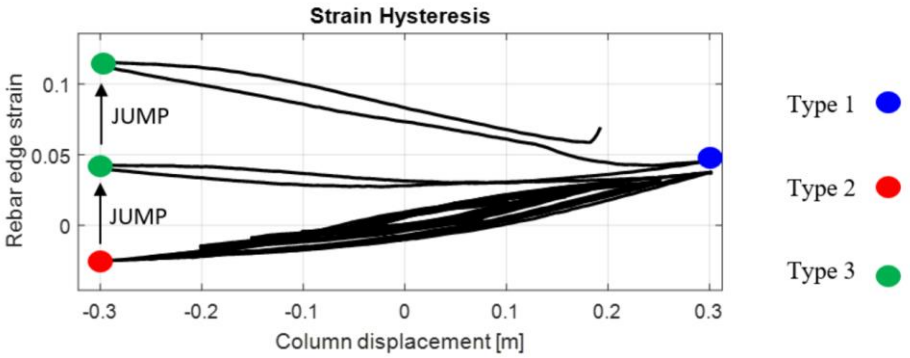

Fig. 2 – Rebar buckling phenomenon in strain hysteresis curves

2.2 Predictive Fiber Model (PFM)

The PFM is a computational model based on fiber and link elements that predicts rebar buckling based on nonlinear material properties, geometric nonlinearities, and deformation compatibility. The PFM is a combination of constraint conditions and fiber elements that gives a convergent, efficient, and accurate representation of the rebar buckling phenomenon. Indeed, PFM assumes that the material properties are well defined by the user, and the utilized software can include the influence of geometric nonlinearities.

Moreover, the PFM also assumes that the user is considering an adequate rotational spring at the base, so the rotations due to strain penetration will be well included in the response. In that way, the PFM just proposes the structural conditions that represent the real deformation compatibility between rebar and concrete at the base of a column.

The main idea that this model uses is the fact that rebar is not a fiber of the RC section when rebar buckling is triggered. Instead, the buckled rebar behaves as an individual fiber element detached from the concrete core. Following this, the first action adopted to develop the PFM is to use fiber elements for the rebar at the base of the column. Based on measurements of the experimental data set, it can be concluded that rebar buckling happens just in the first 0.30 m above the column-foundation interface. Additionally, the fiber element used for the rebar must be an inelastic displacement-based frame element [16] because it permits to have a correct discretization of the rebar and reduces convergence issues in the computational solution.

Once the rebar is modeled as a fiber element at the base of the column, the next conflicts to solve are the connectivity and discretization of the rebar and the concrete core. Regarding the connectivity, the rebar displacements are limited by the ties and the concrete core. The ties control the outward and inward displacement of the rebar while the concrete core limits just the inward displacement of the rebar. Additionally, the rebar and the concrete core must follow the Bernoulli-Euler beam theory (plane sections remain plane). Thus, the rebar and concrete can have different displacements in the outward direction of the column, but the rebar and concrete core must have the same displacements in the longitudinal axis of the column. Moreover, this study considers that the minimum discretization of the rebar is two fiber elements between ties, for it permits to have inflection and control points in the middle of ties. Because of the discretization of the rebar, the concrete core also requires two elements between ties. Indeed, the concrete core elements are very thin, so they must be modeled as inelastic displacement-based frame elements to reduce convergence issues.

Conventional fiber models for columns use a few fiber elements, and the most used type of element is the inelastic force-based frame element. However, because of the buckling phenomenon in the rebar and the aspect ratio of the concrete core elements, displacement-based frame elements are used at the base of the column. The discretization at the base for the PFM requires too many elements, so it affects the computational efficiency. Thus, it is desired to reduce the number of rebar modeled as fiber elements, so it is recommended to model some rebar as fibers at the core section and the others as fiber elements detached from the core. The rebar closest to the neutral axis have smaller strain demand, so they are not likely to experience buckling. Moreover, experimental observations confirm that buckling happens just in the farthest rebar from the neutral axis, so this reduces the number of rebar required as fiber elements. Additionally, this study confirms that the core section must have some tension capacity to improve the convergence of the model, so the core section must have some steel fibers. A graphical comparison between a conventional column and the PFM fiber section is presented in Fig. 3.

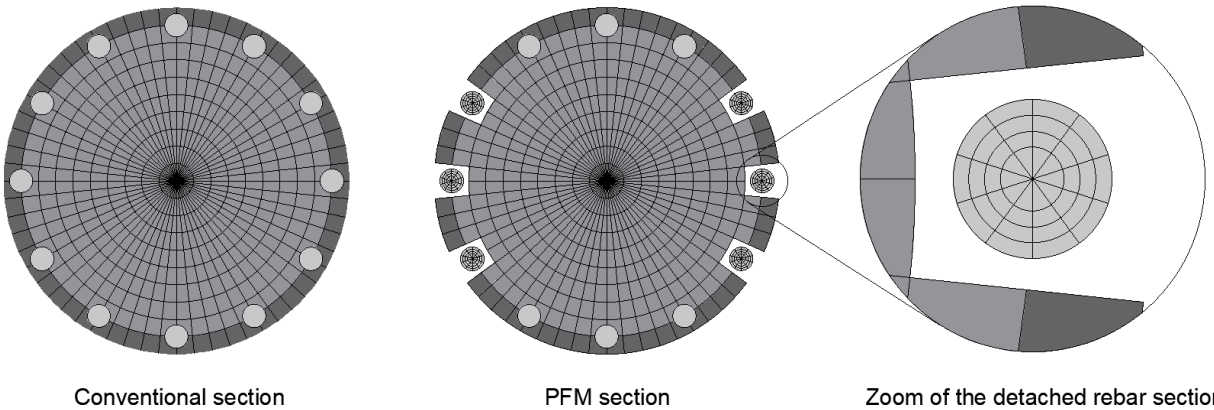

Fig. 3 – Conventional column section versus PFM section

Having identified the boundary conditions, the discretization, and the types of elements, deformation compatibility is achieved by link elements and constraint conditions. Because the PFM uses links of zero length, a connection node is needed at the same location of each rebar node. This connection node helps to include many links between the core and the rebar, so the PFM section can follow the Bernoulli-Euler beam theory and permit the rebar to buckle in the outward direction of the column. First, rigid links are connected between the core node (master node) and connection nodes (slave nodes), so all the nodes connected with rigid links will create a plane section that remains plane. Thus, the connection nodes share the displacements and rotations of the core node affected by the length of the rigid arm. As a result, the connection nodes are ready to be connected with zero-length links to the rebar nodes.

The concrete core restrains the rebar inward displacements, so a contact link with asymmetric elastic properties is used. This contact link has one stiffness for tension and another for compression, so a larger stiffness (10E+10 kN.m) is used for the inward direction and zero stiffness for the outward direction. For large displacement demands, complete cover spalling is expected, and the only elements that provide outward restraint to the rebar are the ties. The boundary conditions provided by the ties can be included with zero-length links at each side of the rebar; the response direction of these tie links can be aligned to the adjacent rebar. Moreover, the tie links should be modeled with a cyclic constitutive model, and this constitutive model must represent the elastic and yielding portion of the steel. Zero-length links have equal strains and displacements, so the tie links should have a yielding displacement equal to the yielding strain of the steel and a yielding strength equal to the rebar section times the yielding stress of the steel. One contact link and two tie links (one for each side) are connecting each connection node with its respective rebar node. Finally, to satisfy the Bernoulli-Euler beam theory, the connection nodes and the rebar nodes must have equal degrees of freedom in the axial direction of the column. A graphical description of the PFM section connectivity is presented in Fig. 4.

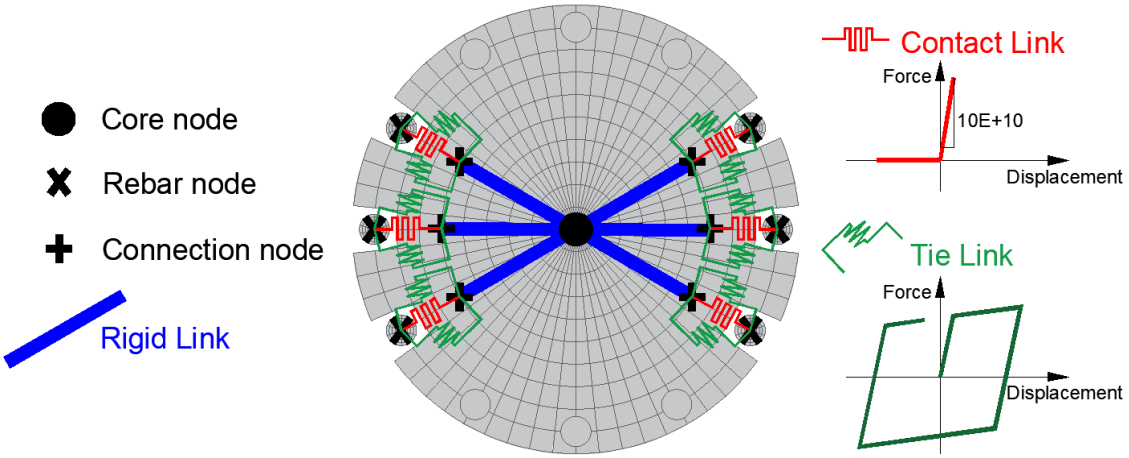

Fig. 4 –PFM section connectivity

2.3 Application

This section illustrates an application that describes the inclusion of the PFM in a standard computer program for structural nonlinear analysis. The experimental data corresponds to specimen #21 tested by [14]; a general description of the materials, geometry, and other structural conditions are presented in Table 1. Specimen #21 is part of a set of large-scale bridge columns subjected to different load histories including monotonic, cyclic, and earthquake time history response tested by [14], and this experimental data is the reference point to validate the PFM. Moreover, the software used for this example is SeismoStruct [16], but the PFM can be implemented in any software that uses the fiber method approach. SeismoStruct was selected because it is an intuitive platform with a graphical interface for structural modeling and data post-processing.

Table 1 – Geometry and materials

Geometry and components	
Description	*Value*
Diameter	432 mm
Cover to longitudinal bars	10 mm
Number of longitudinal bars	10
Diameter of longitudinal bars	20 mm
Diameter of transverse steel	10 mm
Spacing of transverse steel	50 mm
Type of tranverse reinforcement	spirals
Member Length	3353 mm

Material properties and others	
Description	*Value*
Axial load	323 kN
Concrete compressive strength	44 MPa
Long steel yielding stress	470 MPa
Long steel max. stress	637 MPa
Transverse steel yielding stress	452 MPa
Type of concrete	normalweight
Type of displacement	Single Bending
Axial Load Ratio	0.05

The constitutive material used for concrete is the Mander nonlinear model (con_ma) and the Menegotto-Pinto steel model (stl_mp) for reinforcing steel. The core is defined with confined con_ma for the concrete core and stl_mp for the steel fibers closest to the neutral axis (4 fibers). The cover is included with unconfined con_ma, and the rebar furthest from the neutral axis uses fiber elements (6 detached rebar) with stl_mp material. Fig. 5 summarizes the sections of the model, and a 3D view of the discretization of the column is presented to easily identify the base and the upper column regions. Because the spacing between ties is around 5cm, each column and rebar element at the base must be a maximum of 2.5cm tall. In that way, there is at least one control node between ties, so there are 12 column elements and 72 rebar elements (12 elements per detached rebar).

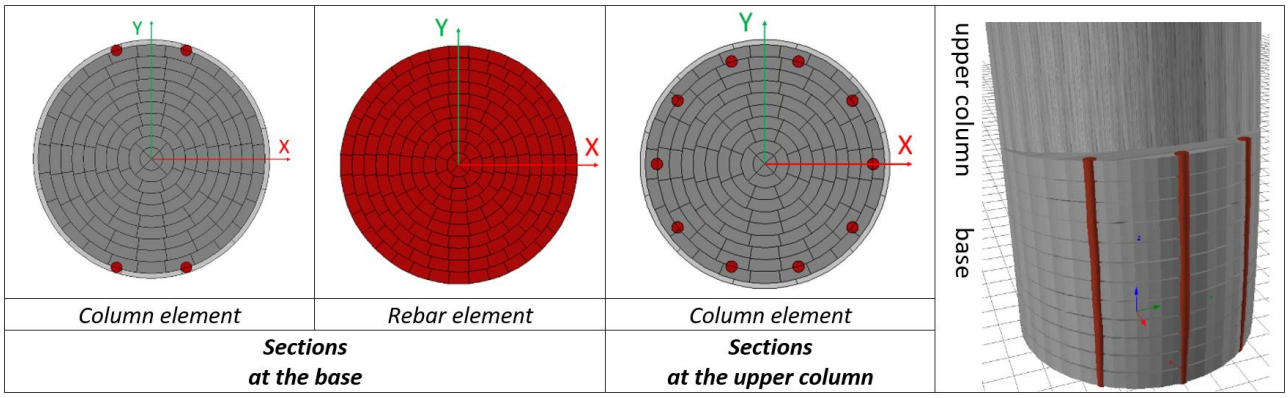

Fig. 5 –Sections of the model [16]

Once the main elements are defined, it is necessary to incorporate the connection nodes. The connection nodes for this example are 6 nodes per-interface from the bottom through the top of the base region; except for the first and the last interfaces in which the rebar is connected directly with rigid links to the core node. Indeed, this completely rigid constraint of the rebar in the first and last interface of the base region provides stability to the rebar. The base region has 66 connection nodes. Then, 6 rigid links are included in each interface to connect the core node (master node) to the connection nodes (slave nodes), resulting in 66 rigid links in total at the base region. Later, the contact links join the connection nodes with the rebar nodes; in this case, there are also 66 contact links. The next elements are the tie links, which are located every two interfaces because the ties have 5cm of spacing. There are two tie links per connection node every two interfaces, resulting in 60 tie links. A column under unidirectional lateral loading is a 2D

structural problem, but buckling has displacements outside of the column. For this reason, the PFM solves a 3D problem, and the response direction of each of the elements used in this model must be well defined.

The contact link is modeled with an asymmetric elastic link, so this link has a large stiffness in one direction (10E+10) and zero stiffness in the other direction. Additionally, the tie link is modeled with a Ramberg-Osgood function to represent the cyclic behavior of the steel material. The yielding strength of the tie link is 35.5 kN, which is equal to the area of the transverse reinforcement times the yielding stress of the steel, and the yielding displacement is equal to the yielding strain of the steel (0.0025) as it is a zero-length link element. Furthermore, a rotational spring must be included at the base, for RC columns have additional rotation due to strain penetration and slip of the rebar at the column-foundation interface. The intention of the PFM is not to propose a bond-slip model, so any available model in the literature can be included for considering this component of deformation. In this particular example, [14] has experimental measurements of the rebar slip at the column-foundation interface, so the rotational spring can be determined experimentally. This spring is a zero-length rotational link where the curvature is equal to the rotation. Therefore, the rotation is calculated as the difference of the rebar slip at each side of the column divided by the diameter of the column. Finally, that rotation is related to the moment produced by the actuator times the height of the column for each step of loading history. The experimental data can be represented with a multilinear spring in SeismoStruct; the calibration of the rotational spring is presented in Fig. 6. The global response is highly dependent on the rotational spring, so this parameter should be carefully defined.

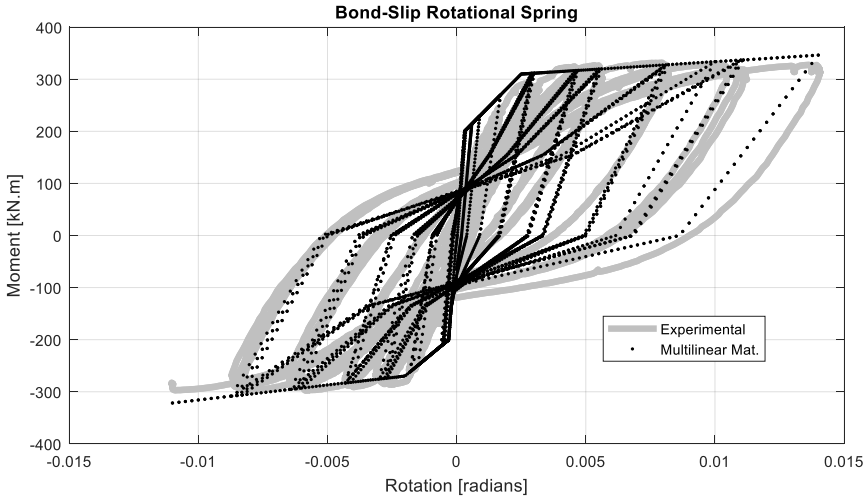

Fig. 6 –Bond-Slip rotational spring

3. Results

The PFM did not present any convergence issues in the SeismoStruct Model, but because it has many conditions and elements the runtime was around 20 minutes for a cyclic pushover of 26 cycles in a conventional desktop. A conventional fiber model has a runtime of a few minutes and can include the effect of buckling. However, conventional models cannot predict rebar buckling, so the additional runtime that the PFM requires is justified to generate the computational data of the rebar buckling phenomenon. Moreover, this section validates the accuracy of the PFM based on the global response of the column and local response of the rebar. The specimen #21, which was explained in section 2.3, presents a good match for the capacity curve and strain hysteresis. A graphical comparison of the capacity curve and strain hysteresis curve for specimen #21 is presented in Fig. 7 and Fig. 8 respectively; this comparison wants to explain the differences between the response obtained with the conventional fiber model versus the PFM. Indeed, both models use the same material properties and bond-slip rotational spring, but the answers are different for the nature of each model.

The capacity curves presented in Fig. 7 show few differences between the prediction obtained with the conventional fiber model and the PFM. For example, the PFM has more pinching effect than the conventional model, and the PFM has a better match of the maximum and minimum base shear for large column displacements. Regardless the capacity curves of both models have a good match compared with the experimental results; the strain hysteresis curves presented in Fig. 8 are completely different between both models for the same rebar and column section. Based on the explanation of the rebar buckling phenomenon in strain hysteresis curves presented in section 2.1 and Fig. 2, it is observed in Fig. 8 that conventional fiber models can predict the strain hysteresis coordinates type 1 and type 2. However, conventional models cannot predict coordinates type 3, so they can not predict rebar buckling. On the other hand, the local strain response of the PFM presented in Fig. 8 includes all the types of strain hysteresis coordinates, for it can predict rebar buckling.

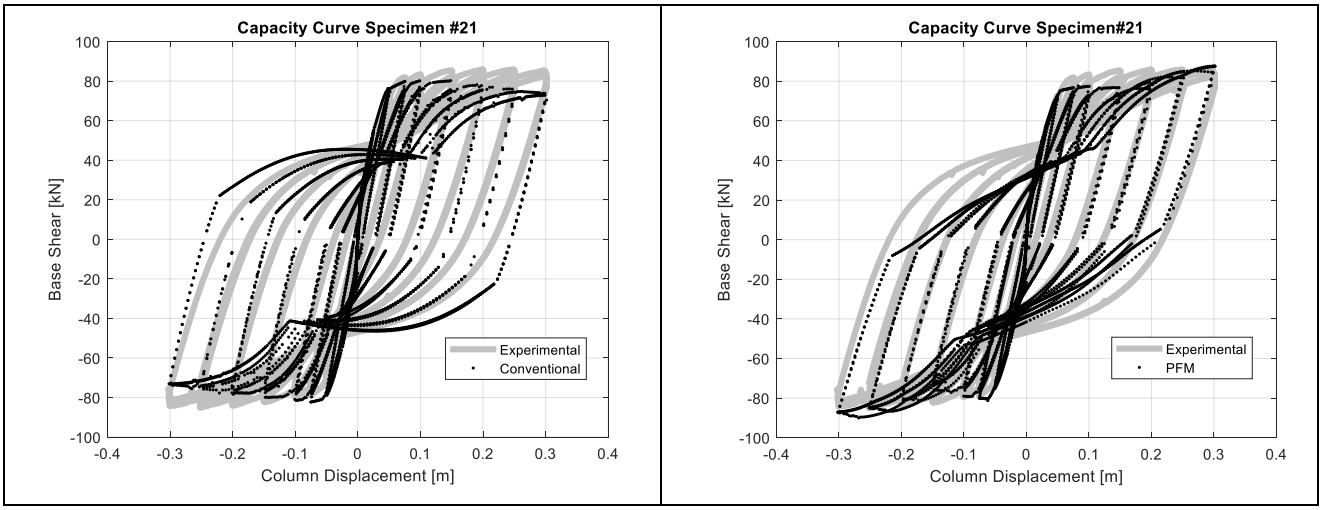

Fig. 7 –Specimen #21 global response prediction

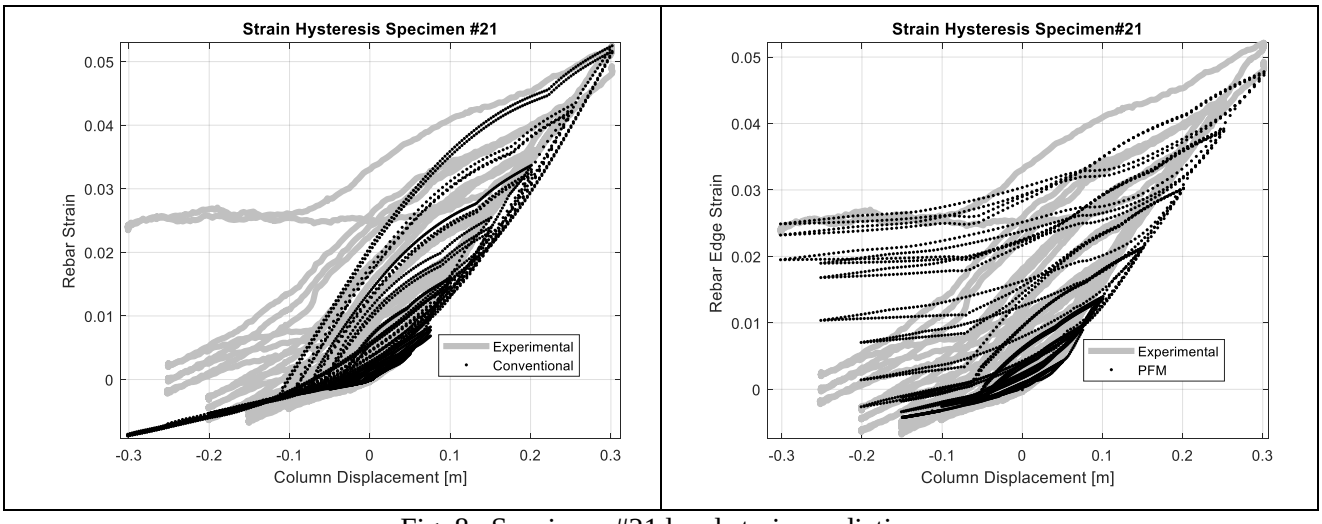

Fig. 8 –Specimen #21 local strain prediction

Table 2 presents the relation between experimental response versus the PFM response for specimen #21 and other 2 specimens; this table compares four parameters: the maximum force-displacement ordinate, the minimum force-displacement ordinate, the energy dissipated, and local strain hysteresis. The force-displacement maximum and minimum ordinates are compared based on the positive and negative shear force

at the base, and the energy dissipation comparison considers the area in a loop of the capacity curve. Moreover, the strain hysteresis compares the tensile and compression strain of a rebar node located at 0.1 m above the column-foundation interface; all four parameters are evaluated to different displacement ductility demands (μ). It can be noticed in Table 2 that the global response has the closest values to 1, and the local response in most of the cases has values under 1.25.

Table 2 – Ratio of the Experimental Response to the PFM Response

Test	μ	Global			Local	
		Base Shear		Energy	Strain	
		Positive	Negative		Tension	Compression
Specimen #19	3	1.05	1.05	0.93	1.45	1.09
	4	1.02	1.04	1.05	1.08	1.07
	5	1.02	1.02	1.03	0.93	0.91
	6	0.97	0.99	1.03	0.8	1.08
Specimen #21	3	1.09	0.99	0.94	1.17	1.12
	4	1.03	0.95	1.02	1.09	1.07
	5	1.01	0.96	1.006	1.13	0.25
	6	1.01	0.97	1.02	1.06	1.004
Specimen #24	3	1.11	1.13	1.1	1.07	3
	4	1.09	1.15	1.14	1.08	1.25
	5	1.03	1.09	1.1	1.03	1.06
	6	0.99	1.05	1.03	1.12	1.17

The PFM represents the kinematics of member deformation and its influence on the rebar buckling phenomenon. In the PFM the rebar are loaded in tension and compression until the rebar buckling is triggered, and after the onset of rebar buckling the PFM captures the progressive evolution of this phenomenon. Fig. 9 shows a graphical representation of specimen #21 response at the last cycle of loading, so the evolution of rebar buckling for this cycle can be observed in this figure. Moreover, Fig. 9 demonstrates that the PFM addresses other phenomena like rebar buckling in many reinforcement bars at the same time, rebar buckling distribution on all the bar length, and permanent rebar buckling at zero displacement of the column.

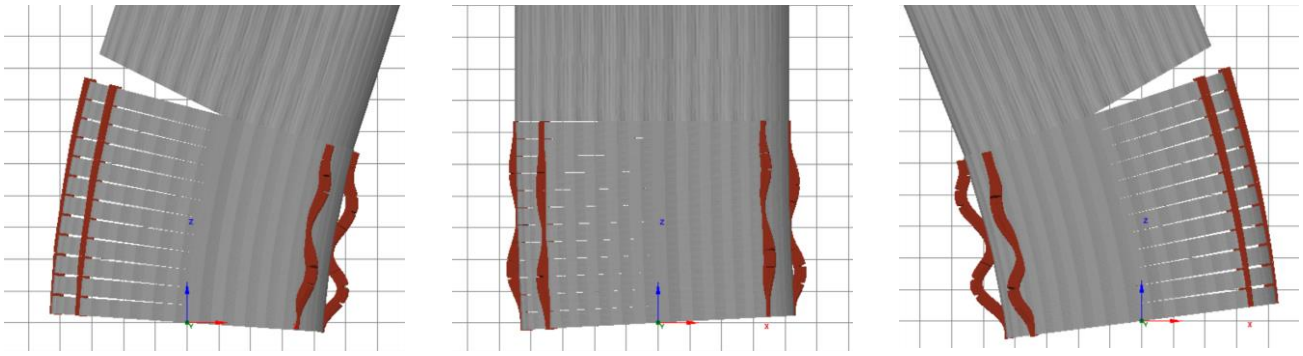

Fig. 9 –Rebar Buckling based on kinematics of member deformation [16]

4. Discussion

The strain hysteresis presented in Fig. 8 shows that the PFM is predicting the three different types of coordinates of the strain hysteresis curve described in section 2.1 and Fig. 2. Indeed, conventional models are able to predict the coordinates type 1 and type 2, but they cannot represent the behavior of type 3. However, PFM has rebar elements detached from the core section, which can represent axial and flexural deformations, so the coordinate type 3 in the strain hysteresis diagram is reproduced by the PFM. Thus, the PFM is predicting the rebar buckling phenomenon in RC columns.

The experimental study developed by [14] provides the local data corresponding to one fiber at the edge of the rebar, and this data helps to calibrate and validate the PFM. Moreover, the columns modeled with the PFM complement the rebar buckling data obtained by [14] because the PFM calculates the response of the other fibers in different sections of the rebar. Additionally, the PFM can calculate the internal actions by the integration of the fibers' response in each section of the rebar fiber elements, so the components (axial and flexural) can be identified independently. Furthermore, following a similar approach than the one presented by [1] and [2], average constitutive models for reinforcing steel with buckling can be developed with the use of the PFM. Indeed, the constitutive models based on the PFM will consider the real boundary conditions for rebar buckling in RC columns under seismic loading.

The current assumptions of the PFM for boundary conditions between the detached rebar and the column core are logical and simple, but there are some improvements that can be implemented in the future to get a better accuracy of the actual proposal. For example, the properties considered for the contact link and tie link should be calibrated based on the local experimental data obtained by [14]. Additionally, the current PFM does not include the column outward pressure due to core expansion, and this condition modifies the onset of buckling. Moreover, the current PFM considers that rebar buckle to the outward direction of the column, but the experimental observations show that rebar can buckle perpendicular to the body of the column, tangent to the column body, or something in between. Finally, there are ongoing studies by the authors of this paper to evaluate the sensitivity of the PFM based on link properties calibration, column core outward pressure, and buckling directionality.

5. Conclusions

The PFM is a group of structural conditions applied at the base of RC columns to predict rebar buckling with the use of the fiber method approach. The PFM predicts the rebar buckling phenomenon in RC columns under cyclic lateral displacements based on deformation compatibility, nonlinear material properties, and geometric nonlinearities. Moreover, the PFM shows that it is an efficient and convergent procedure for rebar buckling modeling, so it can be used in cyclic pushover analyses to reduce the required runtime. Conventional RC fiber models can include the effect of rebar buckling, and they are faster than the PFM. However, those conventional models cannot predict the rebar buckling phenomenon, for they consider the rebar as one fiber in the transverse section of RC columns. Additionally, the PFM captures the influence of the kinematics of the member deformation in the rebar buckling phenomenon, and the PFM represents rebar buckling as a progressive phenomenon in RC columns. The PFM is accurate to represent the global response (capacity curve), but it needs to improve the local buckling prediction (strain hysteresis). To reduce the error in the local buckling prediction, the PFM needs to improve the contact and tie spring models, and it needs to include the expansion of the concrete core and the rebar buckling directionality. Finally, this proposal is an efficient and convergent computational model that implements real boundary conditions between rebar and column core to predict rebar buckling in RC columns under seismic loading.

6. Acknowledgments

This paper and the research behind it would not have been possible without the exceptional support of SENESCYT, EPN, NC State, and CFL.

7. References

[1] Dhakal, R. P., Maekawa, K. (2002a). Modeling for postyield buckling of reinforcement. *Journal of Structural Engineering*, **128**(9), 1139-1147.

[2] Dhakal, R. P., Maekawa, K. (2002b). Path-dependent cyclic stress–strain relationship of reinforcing bar including buckling. *Engineering Structures*, **24**(11), 1383-1396.

[3] Dhakal, R. P., Maekawa, K. (2002c). Reinforcement stability and fracture of cover concrete in reinforced concrete members. *Journal of Structural Engineering*, **128**(10), 1253-1262.

[4] Akkaya, Y., Guner, S., Vecchio, F. J. (2019). Constitutive Model for Inelastic Buckling Behavior of Reinforcing Bars. *ACI Structural Journal*, **116**(2), 195-10.

[5] Girgin, S. C., Moharrami, M., Koutromanos, I. (2018). Nonlinear Beam-Based Modeling of RC Columns Including the Effect of Reinforcing-Bar Buckling and Rupture. *Earthquake Spectra*, **34**(3), 1289-1309.

[6] Zong, Z., Kunnath, S. (2008). Buckling of reinforcing bars in concrete structures under seismic loads. *14h World Conference on Earthquake Engineering*, Beijing, China.

[7] Zong, Z., Kunnath, S., Monti, G. (2013). Simulation of reinforcing bar buckling in circular reinforced concrete columns. *ACI Structural Journal*, **110**(4), 607-616.

[8] Feng, Y., Kowalsky, M. J., Nau, J. M. (2014a). Finite-element method to predict reinforcing bar buckling in RC structures. *Journal of Structural Engineering*, ASCE, 04014147.

[9] Monti, G., and Nuti, C. (1992). Nonlinear Cyclic Behavior of Reinforcing Bars Including Buckling. *Journal of Structural Engineering*, ASCE, 3268-3284.

[10] Rodriguez, M. E., Botero, J. C., and Villa, J. (1999). Cyclic Stress-Strain Behavior of Reinforcing Steel Including Effect of Buckling. *Journal of Structural Engineering*, ASCE, 605-612.

[11] Moyer, M. J., Kowalsky, M. J. (2003). Influence of Tension Strain on Buckling of Reinforcement in Concrete Columns. *ACI Structural Journal*, 75-85.

[12] Bae, S., Mieses, A. M., & Bayrak, O. (2005). Inelastic buckling of reinforcing bars. *Journal of Structural Engineering*, 314-321.

[13] Massone, L. M., Moroder, D. (2009). Buckling modeling of reinforcing bars with imperfections. *Engineering Structures*, **31**(3), 758-767.

[14] Goodnight, J. C., Kowalsky, M. J., Nau, J. M. (2013). Effect of load history on performance limit states of circular bridge columns. *Journal of Bridge Engineering*, **18**(12), 1383-1396.

[15] Northern Digital, Inc., 2015. OPTOTRAK Certus HD Dynamic Measuring Machine, Products, available at http://www.ndigital.com/industrial/certushd.php.

[16] Seismosoft (2018) "SeismoStruct 2018 – A computer program for static and dynamic nonlinear analysis of framed structures," available from http://www.seismosoft.com.

